Dyes and Pigments 92 (2011) 737–744

Contents lists available at ScienceDirect

Dyes and Pigments

journal homepage: www.elsevier.com/locate/dyepig

Dichroic and spectral properties of anthraquinone-based azo dyes for PVA polarizing film

Jae Bok Chang [a], Sim Bum Yuk [a], Jong S. Park [b], Jae Pil Kim [a,*]

[a] *Department of Materials Science and Engineering, Seoul National University, Seoul 151-744, Republic of Korea*
[b] *Department of Polymer & Textile Industry, Dong-A University, Busan 604-714, Republic of Korea*

ARTICLE INFO

Article history:
Received 19 March 2011
Received in revised form
26 May 2011
Accepted 2 June 2011
Available online 6 July 2011

Keywords:
Anthraquinone
Bichromophore
Charge transfer transition
Dichroic ratio
Polarizing films
Transition moment

ABSTRACT

Dichroic dyes with broad absorption bands are advantageous for the production of neutral gray polarizing films. For this purpose, anthraquinone-based azo dyes were synthesized to have a conjugated bichromophore design and this was applied to PVA polarizing films. The spectral and dichroic properties of the polarizing films were examined and compared to the films produced with a general disazo dichroic dye. The polarizing films with anthraquinone-based azo dyes had wider absorption bands, but lower dichroic ratios compared to the films with a general disazo dichroic dye. It was found that the alignment between the transition moments of the anthraquinone and azo chromophores is an important factor for the dichroic properties of anthraquinone-based azo dyes.

1. Introduction

The polarizing films are linear polarizers that absorb light in one particular vibration direction. Commercial polarizing films for liquid crystal displays (LCDs) are manufactured from oriented poly(vinyl alcohol) films containing polarizing materials, such as iodine or dichroic dyes. Iodine types have superior transmittance and polarizing efficiency but they are vulnerable to heat and humidity [1–3]. In contrast, dye types have inferior optical properties compared with iodine types but they have higher resistance to heat and humidity [4–6]. As the flat panel display market grows and the demand for highly durable polarizing film increases, dye types are gaining more industrial attention.

Poly azo dyes are the most widely used class of dyes for polarizing films because they are advantageous in adsorption on PVA and they achieve higher dichroism due to their linear structure and anisotropic transition moment. Generally, poly azo dyes have narrower light absorption bands compared to iodine anions (I_3^- and I_5^-) [7,8]. Therefore, various dyes of different colors should be appropriately blended for the even absorption of visible light. This color matching for neutral gray becomes complicated when the number of dyes used increases. Therefore, broadening of absorption ranges of dyes is helpful for easier color matching and higher color reproducibility. However, recent studies have mostly been focused on the improvement of transmittance and polarizing efficiency of dye type polarizing film [4–8].

In this study, anthraquinone-based azo dyes, which have an anthraquinone and two azo chromophores, were designed and synthesized for dichroic dyes with broader absorption spectra than the dyes used in our previous work [9]. PVA polarizing films were produced with the dyes, and their spectral and dichroic properties were examined and compared with those of the disazo dye (DA).

2. Experimental

2.1. Materials and instrumentation

1,5-Diamino-anthraquinone and 2,6-diamino-anthraquinone were purchased from Sigma–Aldrich and 7-amino-4-hydroxy-2-naphthalenesulfonic acid (J-acid) and 4-amino-acetophenone were obtained from TCI. All other chemicals used in this study were of synthesis grade. Poly(vinyl alcohol) film was supplied by Kuraray Co. Ltd., with degree of polymerization of 2400, a degree of saponification of 99.9% and its thickness was 75 μm.

---

* Corresponding author. Tel.: +82 2 880 7187; fax: +82 2 880 7238.
E-mail address: jaepil@snu.ac.kr (J. P. Kim).

0143-7208/$ – see front matter Crown Copyright © 2011 Published by Elsevier Ltd. All rights reserved.
doi:10.1016/j.dyepig.2011.06.024

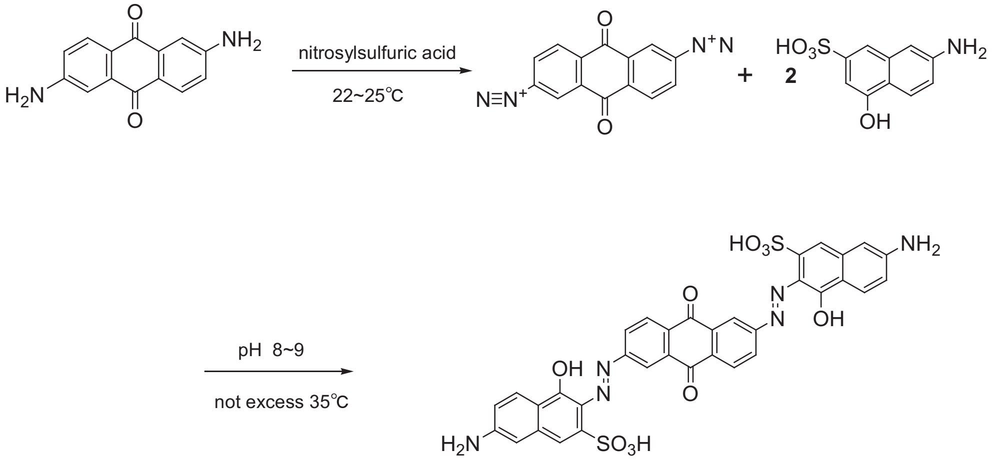

Scheme 1. Synthesis of 26B.

The ^1H NMR spectra were recorded on a Bruker Avance 500 spectrometer using DMSO-d_6 and TMS as the solvent and the internal standard, respectively. The FT-IR spectra were recorded on a Thermo Scientific Nicolet 6700 using ATR method. The mass spectra were recorded in fast atom bombardment (FAB) ionization mode using a JEOL JMS-AX505WA/HP 6890 Series II Gas Chromatography-Mass Spectrometer. The absorption spectra were measured on an HP 8452A spectrophotometer which was equipped with a Glan-Thompson polarizer. The color differences of the polarizing films were analyzed using a Scinco Colormate.

2.2. Synthesis of dyes

2.2.1. Synthesis of anthraquinone-based azo dyes

Anthraquinone-based azo dyes were synthesized as shown in Scheme 1. 2,6-Diamino-anthraquinone (1.43 g, 0.006 mol) were slowly introduced into concentrated sulfuric acid (10 mL) and temperature of the mixture was kept below 40 °C. After stirring for 30 min at room temperature, 40% nitrosyl sulfuric acid (2.6 mL) was added dropwise maintaining the mixture at room temperature. The mixture was stirred for 4 h at room temperature and then it was quenched with ice water (140 mL). After stirring for 30 min, the

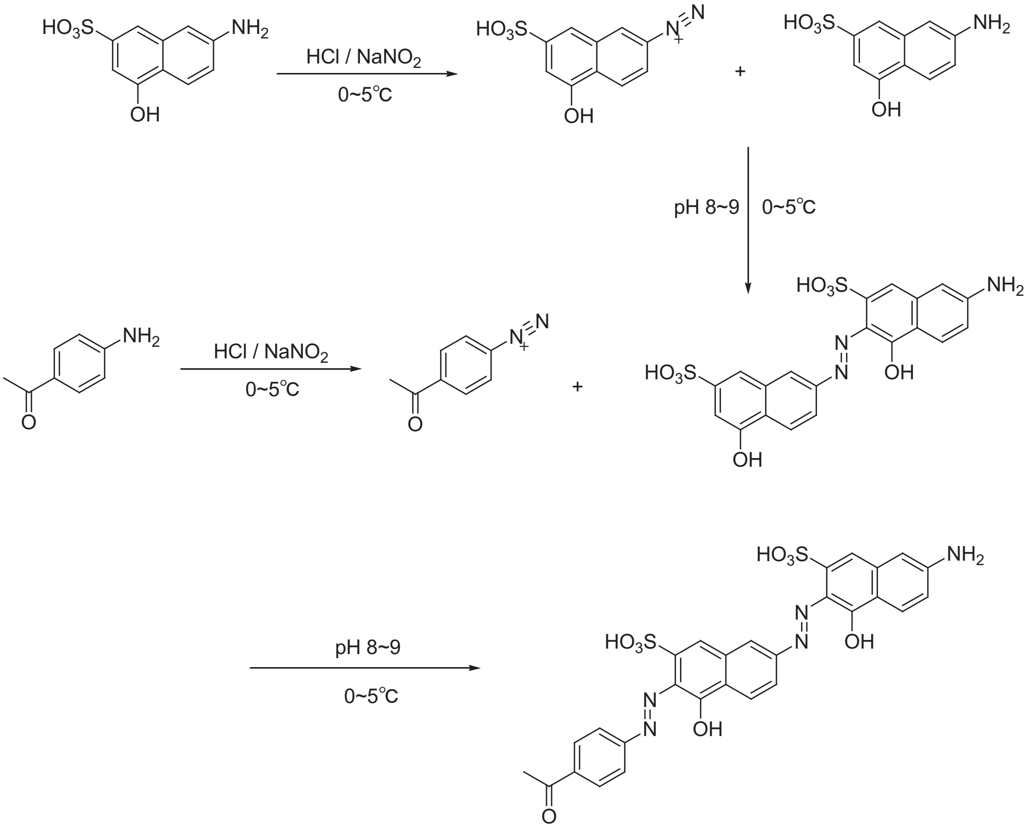

Scheme 2. Synthesis of DA.

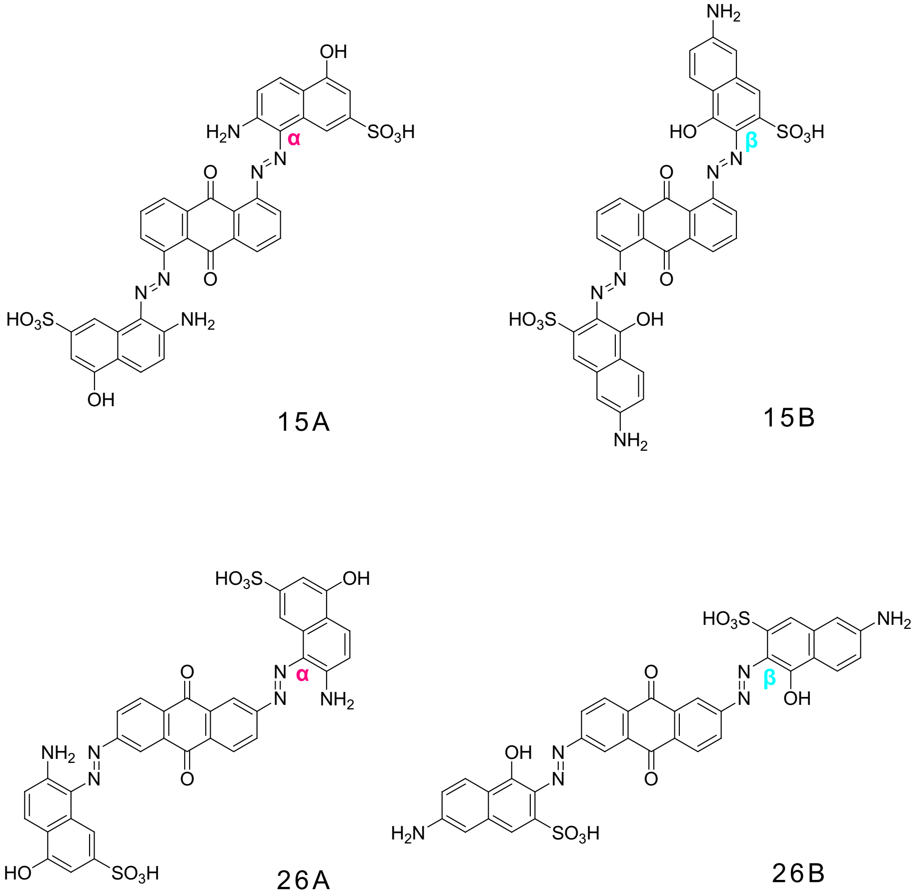

Fig. 1. Structures of anthraquinone-based azo dyes.

diazonium salts were obtained by filtration of the mixture. The diazonium salts were added to 30 mL of water with 5 mL of 2 M hydrochloric acid and the mixture was stirred for 30 min. The ensuing mixture was dropped into a solution of 7-amino-4-hydroxy-2-naphthalenesulfonic acid (2.87 g, 0.012 mol) dissolved in water (100 mL) for coupling reaction. In the course of dropping, the temperature and pH of the mixture were maintained at 0–5 °C and 9–10, respectively. The reaction mixture was stirred for 2 h at 0–5 °C and then another 5 h at room temperature. The mixture was acidified with 2 M hydrochloric acid and the precipitate was collected by filtration. The crude product (26B) was washed with brine and ethanol and dried in a vacuum oven. The other anthraquinone-based azo dyes were prepared in a similar manner.

2.2.2. Synthesis of disazo dye

A disazo dye (DA) was synthesized as shown in Scheme 2. 7-Amino-4-hydroxy-2-naphthalenesulfonic acid (2.65 g, 0.01 mol) was dissolved in water (50 mL) at room temperature and pH of the solution was adjusted to 7.0 by adding 10% sodium carbonate solution. The solution was cooled to 0–5 °C and 2.5 mL of 2 M aq sodium nitrite was added dropwise. The ensuing solution was dropped into 2 M hydrochloric acid (50 mL) and stirred for 1 h, after which time, a small portion of sulfamic acid was added as a nitrous acid scavenger. The resulting diazonium salt solution was added to a coupling component solution of 7-amino-4-hydroxy-2-naphthalenesulfonic acid (2.65 g, 0.01 mol) dissolved in water (80 mL), while the temperature and pH of the mixture were

Table 1
Yield, ^{1}H NMR and mass data of the synthesized dyes.

Dye	Yield (%)	^{1}H NMR (ppm, DMSO-d_6)	Mass (m z–^{1}, 100%, $[M+H]^+$)
15A	81.3	7.08 (s, 2H, NH), 7.95 (s. 2H, ArH), 8.01 (d, $J = 8.5$ Hz, 2H, ArH), 8.28 (d, $J = 8.6$ Hz, 2H, ArH), 8.31 (t, $J = 8.1$ Hz, 2H, ArH), 8.40 (s, 2H, ArH), 8.45 (d, $J = 7.4$ Hz, 2H, ArH), 8.65 (d, $J = 7.8$ Hz, 2H, ArH), 10.13 (s, 2H, OH), 13.92 (s, 2H, NH)	738.08
15B	82.4	6.89 (s, 4H, NH_2), 7.55 (s, 2H, ArH), 7.66 (d, $J = 8.4$ Hz, 2H, ArH), 7.74 (d, $J = 8.6$ Hz, 2H, ArH), 7.94 (s, 2H, ArH), 8.18 (t, $J = 8.0$ Hz, 2H, ArH), 8.21 (d, $J = 7.5$ Hz, 2H, ArH), 8.33 (d, $J = 7.9$ Hz, 2H, ArH), 15.81 (s, 2H, OH)	738.08
26A	83.1	7.17 (s, 2H, NH), 7.45 (s, 2H, ArH), 7.65 (d, $J = 8.3$ Hz, 2H, ArH), 7.73 (d, $J = 8.5$ Hz, 2H, ArH), 7.98 (s, 2H, ArH), 8.15 (s, 2H, ArH), 8.29 (d, $J = 7.4$ Hz, 2H, ArH), 8.30 (d, $J = 7.7$ Hz, 2H, ArH), 10.89 (s, 2H, OH), 12.54 (s, 2H, NH)	738.08
26B	81.6	6.67 (s, 4H, NH_2), 7.56 (s, 2H, ArH), 7.69 (d, $J = 8.3$ Hz, 2H, ArH), 7.78 (d, $J = 8.4$ Hz, 2H, ArH), 8.01 (s, 2H, ArH), 8.18 (s, 2H, ArH), 8.26 (d, $J = 7.5$ Hz, 2H, ArH), 8.45 (d, $J = 7.8$ Hz, 2H, ArH), 16.01 (s, 2H, OH)	738.08
DA	67.8	6.55 (s, 2H, NH_2), 6.66 (s, lH, ArH), 6.69 (d, $J = 8.6$ Hz, lH, ArH), 7.29 (s, 1H, ArH), 7.51 (s, 1H, ArH), 7.80 (s, 1H, ArH), 7.82 (d, $J = 8.4$ Hz, 2H, ArH), 7.87 (d, $J = 8.1$ Hz, 1H, ArH), 7.93 (d, $J = 9.5$ Hz, 1H, ArH), 7.98 (d, $J = 8.7$ Hz, 1H, ArH), 8.24 (d, $J = 9.1$ Hz, 2H, ArH), 15.7 (s, lH, OH), 15.9 (s, lH, OH)	635.08

Table 2
Spectral properties of the synthesized dyes.

Dye	λ_{max}[a] (nm)	ε_{max}[a] ($L\,mol^{-1}\,cm^{-1}$)	Half-band width[a] (nm)	λ_{max}[b] (nm)	Half-band width[b] (nm)
15A	534	21,000	234	576	172
15B	528	22,000	230	548	176
26A	526	21,000	228	580	154
26B	538	23,000	205	534	158
DA	532	31,000	95	556	90

[a] In water.
[b] In PVA film.

maintained at 0–5 °C and 8–9, respectively, in the course of the addition. The reaction mixture was stirred for 2 h and the precipitate was filtered, washed with brine and dried in a vacuum oven. The intermediate was heated in ethanol for 2 h under reflux, hot filtered, washed with hot ethanol and then dried in a vacuum oven.

A mixture of 4-amino-acetophenone (0.54 g, 0.004 mol), 2 M aq hydrochloric acid (36 mL) and sodium nitrite (0.28 g, 0.004 mol) was stirred for 1 h at 0–5 °C. To this solution, a small portion of sulfamic acid was added as a nitrous acid scavenger. The resulting diazonium salt solution was added to a coupling component solution where the intermediate (2.14 g, 0.004 mol) was dissolved in water (150 mL) while the temperature and pH of the mixture were maintained at 0–5 °C and 8–9, respectively, in the course of the addition. After coupling, the solution was stirred for 2 h and the precipitate was filtered, washed with brine and dried in a vacuum oven. The crude product (DA dye) was refluxed in ethanol for 2 h, hot filtered, washed with hot ethanol and then dried in a vacuum oven.

2.3. *Preparation of polarizing films*

Dye baths were prepared with a dye (0.5 g), Na_2SO_4 (1.5 g) and distilled water (1 L). PVA films (50 × 70 mm) were treated in the dyeing solution for 6 min at 40 °C. The dyed PVA films were drawn 6 times in 2wt% of boric acid solution at 50 °C. The stretched films were washed with water and dried in an oven for 10 min.

2.4. *Investigation of optical properties of polarizing films*

The optical properties of the polarizing films were measured with a UV–vis spectrophotometer equipped with a Glan-Thompson polarizer. Dichroic ratio (R), single-piece transmittance (T_{sp}) and polarizing efficiency (PE) were evaluated at the absorption maximum of the polarizing films according to Eqs. (1)–(3) [10].

$$R = A_{\parallel}/A_{\perp} \tag{1}$$

$$T_{sp} = \left(T_{\parallel} + T_{\perp}\right)/2 \tag{2}$$

$$PE = \left\{\left(T_{\perp} - T_{\parallel}\right)/\left(T_{\perp} + T_{\parallel}\right)\right\}^{1/2} \tag{3}$$

where $A_{\parallel}$ and $A_{\perp}$ are parallel and perpendicular absorbance to the drawing direction, respectively. $T_{\parallel}$ and $T_{\perp}$ were calculated from the absorbance ($T = 10^{-A}$).

2.5. *Molecular orbital (MO) calculation*

CACHe 6.1.8 software package [11] was used in order to optimize the geometry of dye structures by using molecular mechanics MM3, conducting the iterative energy-minimizing routines with the conjugate gradient minimizer algorithm [12]. CONFLEX conformational search procedure was used for finding low-energy conformations of the dye molecules [13]. The semi-empirical method, PM5, was also examined with respect to geometry optimization. On optimization of conformers, the dye molecules were assumed to have azo linkages in the *trans* forms.

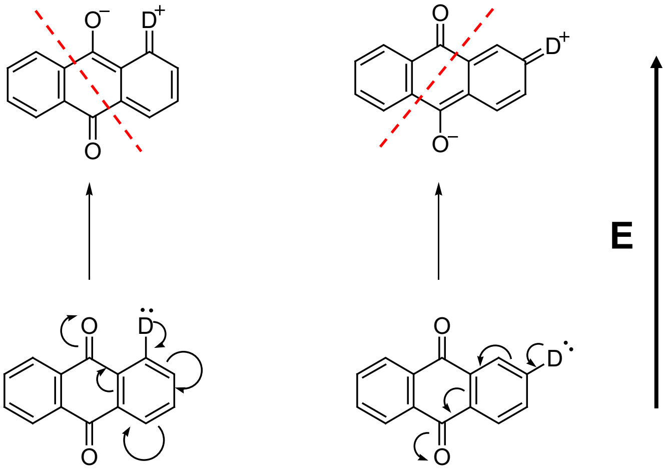

Fig. 2. Charge transfer transitions of 1,5- and 2,6-substituted anthraquinone.

Aspect ratios (*l*/*d*) of dye molecules were calculated from the geometry of the most stable conformer optimized by CONFLEX/MM3 calculation in consideration of van der Waals radius, where *l* and *d* represent the length of the long axes and diameter of the circumscribed cylinders of the dye molecules, respectively. Directions of the transition dipole moments of the dichroic dyes were examined by INDO/1 in the ZINDO package [14] using the dye structures optimized by the above-mentioned calculation. Configuration interaction (CI) calculation up to 676 configuration functions was performed by adapting the occupied orbitals of (HOMO − 25 to HOMO) and the vacant orbitals of (LUMO to LUMO + 25). Each configuration function was generated through the single excitation (S-CI) from the ground-state function [15,16].

3. Results and discussion

3.1. *Structure of synthesized dyes*

Anthraquinone-based azo dyes have azo groups conjugated with anthraquinone, as shown in Fig. 1. 15A and 15B were synthesized by using 1,5-diamino-anthraquinone as a diazo component and J-acid as a coupling component. The position of coupling depended on the pH of the coupling reaction mixture. The coupling of 15A was induced to take place at the ortho position of the amino group (α-position) of J-acid by coupling it under acidic conditions. The coupling reaction of 15B proceeded in alkaline conditions to induce coupling at ortho position of the hydroxyl group (β-position). For

Table 3
Aspect ratio and optical properties of the polarizing films at the absorption maximum of each dye.

Dye	Aspect ratio	R	T_{SP} (%)	PE (%)
15A	2.46	14.12	36.14	98.80
15B	2.71	14.29	35.43	99.09
26A	2.40	15.21	38.13	98.33
26B	3.16	15.14	36.34	99.04
DA	2.70	24.68	39.52	99.65

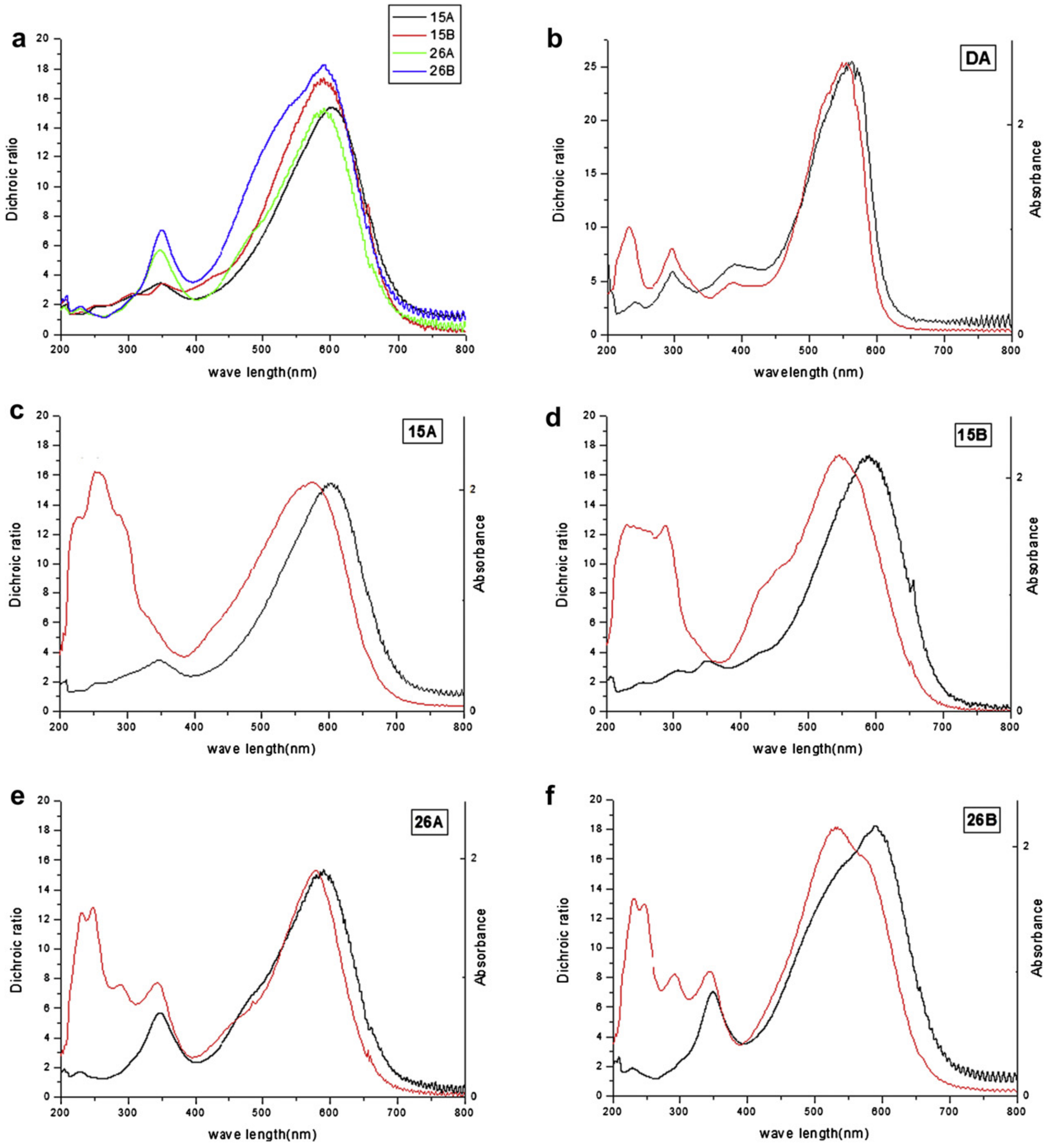

Fig. 3. (a) Dichroic ratio spectra of anthraquinone-based azo dyes and dichroic ratio (black line) and absorption (red line) spectra of (b) DA, (c) 15A, (d) 15B, (e) 26A and (f) 26B. (For interpretation of the references to color in this figure legend, the reader is referred to the web version of this article.).

26A and 26B, the diazonium salt of the 2,6-diamino-anthraquinone was coupled to the α and β-position of the J-acid, respectively.

DA was prepared as a reference for comparison with anthraquinone-based azo dyes. DA has a disazo structure which is common for dichroic dyes and its azo linkages are arranged linearly by coupling at the β-position of the J-acid (Scheme 2). Also, a terminal acetophenone moiety is introduced in DA to make it similar to the chromophore unit of anthraquinone.

The azo linkages of the synthesized dyes existed predominantly in the hydrazone form due to intramolecular hydrogen bonding with an adjacent amino or hydroxyl group. This was confirmed by the down fielded proton peaks (12.5–16.0 ppm) of amino and hydroxyl groups in the ^{1}H NMR data of Table 1 [17].

3.2. Spectral properties of the dyes and PVA polarizing films

The spectral properties of synthesized dyes in water and PVA film are presented in Table 2. The dyes in water had maximum absorption wavelengths of 526–538 nm with magenta shades. Anthraquinone-based azo dyes exhibited similar molar extinction coefficients ranging from 21,000 to 23,000 L mol^{-1} cm^{-1}, whereas DA had higher tinctorial strength ($\varepsilon_{max} = 31{,}000$ L mol^{-1} cm^{-1}). Half-band widths of anthraquinone-based azo dyes in water were more than 200 nm, whereas that of DA was only 95 nm.

The spectral properties of anthraquinone-based azo dyes in PVA film showed a clear dependence on the structure of the dye. 15A and 26A exhibited bathochromic shifts of more than 40 nm in the

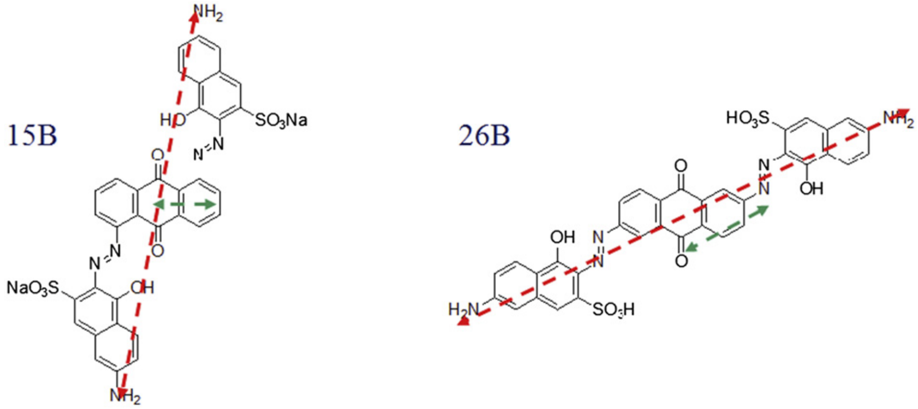

Fig. 4. Schematic diagrams of the orientations of the transition moments of the anthraquinone and azo chromophores in 15B and 26B.

PVA film whereas 15B and 26B had relatively small spectral changes. While the absorption maxima of dyes in the PVA film depended on the position of the coupling of the J-acid, half-band widths were influenced by the position of coupling at the anthraquinone. 15A and 15B had relatively wider half-band widths than 26A and 26B.

The absorption maxima of dyes appear to be determined primarily by the charge transfer of the azo chromophore, which consists of a donor (J-acid), a conjugated system (azo linkage) and an acceptor (anthraquinone). This fact is supported by the distinction between the absorption maxima of the dyes coupled at the α-position and at the β-position. An azo chromophore absorbs a longer wavelength, as the electron-donating power of the adjacent substituent increases [18]. Therefore, 15A and 26A were more bathochromic than 15B and 26B due to the stronger electron-donating power of the amino group compared to the hydroxyl group. Unlike the donor part, the difference of the acceptor part seems to have relatively little influence on the absorption maxima of the dyes. This is because anthraquinones act as acceptor parts with similar levels of electron-withdrawing ability. Carbonyl groups of anthraquinone in 1,5-disubstituted dyes are located on the ortho or meta positions relative to the azo linkage, and carbonyl groups in 2,6-disubstituted dyes are located on the meta or para positions relative to the azo linkage. It is known that electron-withdrawing groups exert a similar inductive effect on the color of the azo chromophore when they are situated on the ortho or para position relative to the azo linkage [18].

Anthraquinone in this study acted as a chromophore as well as an acceptor for the azo chromophore. However, an anthraquinone chromophore typically has a lower tinctorial strength than an azo chromophore [18]. Also, the anthraquinone chromophores of the synthesized dyes are supposed to absorb around the mid-400 nm wavelength range while the absorption band of azo chromophore lies around the mid-500 nm wavelength range. Therefore, the anthraquinone chromophores did not change the absorption maxima of the dyes, which were determined by the azo chromophores, but they broadened the absorption spectra of the dyes by additional absorption in the shorter wavelength range.

As shown in Fig. 2, 1,5- and 2,6-disubstituted anthraquinones had different charge transfer transitions and 1,5-disubstituted anthraquinones are known to be generally more bathochromic and tinctorially stronger than 2,6-disubstituted anthraquinones [18]. Therefore, additional absorption by 1,5-disubstituted anthraquinones could be higher and closer to the absorption maxima compared to that achieved by 2,6-disubstituted anthraquinones. As a result, the dyes have distinctively wide half-band widths depending on the coupling position of the anthraquinone.

3.3. Dichroic properties of anthraquinone-based azo dyes in PVA polarizing films

The linearity of dye molecules could be used as an index for the comparison of their dichroic properties when dyes have chromophores of similar structures, as reported in our previous work [9]. However, the linearity of anthraquinone-based azo dyes, denoted as aspect ratio, seems to bear no relation to the dichroic ratio at the absorption maxima, as shown in Table 3. In the case of DA, the comparison of its dichroic ratio to other dyes is meaningless because of the differences in the structures of chromophores. When dyes have different chromophores, their dichroic ratios are more greatly influenced by other factors, such as the strength and direction of transition moment, than by their aspect ratios. However, this cannot explain the disagreement between the aspect ratio and dichroic ratio in anthraquinone-based azo dyes. The reason for this unexpected result could be accounted for by studying the dichroic ratios of the PVA polarizing film throughout the whole visible region.

Dichroic ratios of anthraquinone-based azo dyes in a PVA polarizing film throughout the whole visible region are depicted in Fig. 3(a). For all anthraquinone-based azo dyes, their maximum dichroic ratios were obtained at longer wavelengths than their absorption maxima. The maximum dichroic ratios of 15A, 15B, 26A and 26B were 15.46, 17.57, 15.52 and 18.35, respectively. When these values were compared to those of their aspect ratio, they were in good agreements. The wavelengths for the maximum dichroic ratio and their difference with the absorption maxima were 598, 586, 590

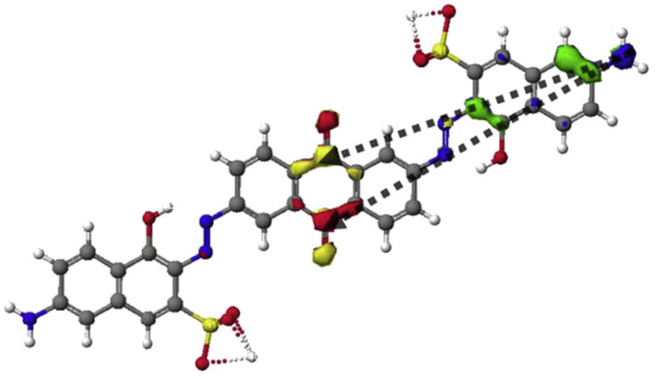

Fig. 5. Charge distribution at HOMO (blue and green electron clouds) and LUMO (red and yellow electron clouds) level of 26B. (For interpretation of the references to color in this figure legend, the reader is referred to the web version of this article.).

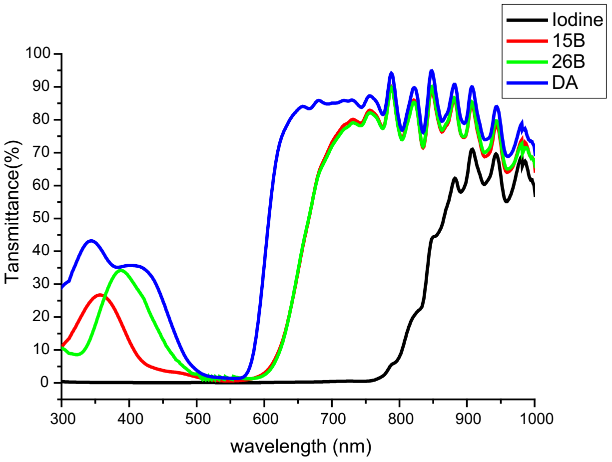

Fig. 6. Cross transmittances of the polarizing films.

and 592 nm and 22, 38, 10 and 58 nm, respectively, for 15A, 15B, 26A and 26B. This discrepancy between the absorption maxima and maximum dichroic ratio is noticeable since the dichroic ratios of general dichroic dyes, such as DA, are almost consistent with their absorption spectra, as shown in Fig. 3(b).

To investigate the transition moment of each chromophore, the maximum heights of the dichroic ratio spectrum and absorption spectrum were set equal and they are depicted in Fig. 3(c)–(f). In the wavelength region below the absorption maxima, 1,5-substituted dyes had lower dichroic ratios compared to absorbance, while 2,6-sustituted dyes had similar values. This difference is believed to be caused by the disagreement of the directions of the transition moments of anthraquinones. As mentioned before in Fig. 2, the direction of charge transfer in 1,5- and 2,6-sustituted anthraquinone chromophores are different. The different charge transfers lead to changes in the direction of the transition moment. Consequently, the direction of the transition moment of the anthraquinone chromophore would be perpendicular to the molecular axis in 1,5-substituted dyes and parallel in 2,6-substituted dyes as shown in Fig. 4. The deviated transition moment of the anthraquinone chromophore in 1,5-substituted dyes resulted in the increase of perpendicular absorbance and thus lowered the dichroic ratio in the shortwave region with respect to absorbance.

The absorptions of 1,5-substituted dyes are caused by two chromophores: anthraquinone chromophore with a lower dichroic ratio absorbs the shorter wavelength region and the azo chromophore with a higher dichroic ratio absorbs in the longer wavelength region. Within the overlapping absorption region of the anthraquinone and azo chromophore, the absorbance can increase but the dichroic ratio will decrease since absorbances are obtained by the sum of each contribution, but dichroic ratios are calculated by averaging their values. Therefore, the dichroic ratio at the absorption maxima would be lower than the dichroic ratio of the azo chromophore itself. For these reasons, 15-substituted dyes had the discordance of absorption maxima and maximum dichroic ratios.

The dichroic ratio curve of the 2,6-substituted dyes were more similar to their absorbance curve in the shortwave region owing to the parallel transition moment of anthraquinone. However, there is still some discrepancy in the wavelengths of absorption maxima and maximum dichroic ratios. This result suggests that the dichroic characteristic of the anthraquinone-based azo dyes is further affected by factors other than the overlapping of the absorption of anthraquinone and azo chromophore.

Fig. 5 shows the charge density distribution of 26B as prepared by molecular modeling. Blue and green clouds on the J-acid are the electron rich parts in the ground state and the red and yellow clouds on anthraquinone are the electron rich parts in the excited state of the dye. When anthraquinone acts as an acceptor of the azo chromophore, the resonance energy transfer pathway of the excited electron will branch off into two directions. This pathway would depend on the energy state of the absorbed light and thus the direction of the transition moment should be subject to change with the wavelengths of absorption. In anthraquinone-based azo dyes, the transition moment beyond the absorption maxima is believed to have a smaller deviation angle relative to the molecular long axis than the angle at the absorption maxima. Accordingly, the maximum dichroic ratio was observed in longer wavelengths than the absorption maxima.

3.4. *Advantage for neutral gray*

The cross transmittance of a pair of polarizing films was measured for films dyed with 15B, 26B, DA and iodine. As shown in Fig. 6, the iodine type absorbed evenly throughout the visible range but the dye types absorbed in limited regions within the visible range. The absorption regions of the anthraquinone-based azo dyes were broader than that of DA.

The broadness in the longer wavelength region is likely due to the acceptor effect of anthraquinone. When an anthraquinone acts as an acceptor of the azo chromophore, their two-way electron-

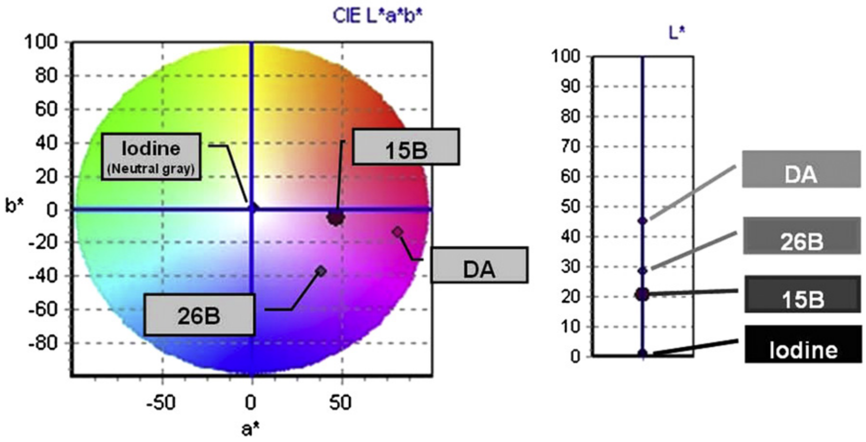

Fig. 7. Color difference on $L^*a^*b^*$ color space CIE1976 and luminance of the polarizing films.

withdrawing effect that was explained previously would allow various excited state π-electrons distributions and this will lead to increases in the bathochromic absorption of the dye.

Difference of transmittance in the shortwave range between 15B and 26B is caused by the different tinctorial strength of anthraquinone chromophores. The wavelengths ranging from 400 nm to 450 nm leaked more on 26B than they did on 15B. This different light leakage related to the shades of the dyes, as shown in Fig. 7. In the $L^*a^*b^*$ color space, 15B and 26B had closer color coordinates to neutral gray than DA.

4. Conclusions

The introduction of the conjugated bichromophore system in a dichroic dye was found to be very effective for increasing the absorption bandwidth. The broad absorption spectra of anthraquinone-based azo dyes are influenced not only by merging different absorptions of anthraquinone and azo chromophores but also by the acceptor effect of anthraquinone. The anthraquinone acted as an acceptor of the azo chromophore and led to broader and bathochromic absorption of azo chromophore due to its various transient energy states. Accordingly, anthraquinone-based azo dyes had a favorable color shade for producing neutral gray polarizing films.

Anthraquinone-based azo dyes had lower dichroic ratios in comparison with general poly azo dichroic dyes such as DA due to the misalignment of transition moments depending on absorption band. The difference between the transition moments of anthraquinone and azo chromophores reduces dichroic ratios in overlapping absorption bands. The transition moment of azo chromophore is attenuated by acceptor effect of anthraquinone because two electron-withdrawing groups of anthraquinone share the charge density of the excited state. These facts could be confirmed by analysis of the discrepancy in the wavelengths between the absorption maxima and maximum dichroic ratio. The findings of this work are expected to provide a useful information about the correlation between dichroic ratio and transition moment.

Acknowledgment

This work was supported by a research grant from Ministry of Knowledge Economy (MKE, No. 10030016).

References

[1] Lyoo WS, Yeum JH, Ghim HD, Park JM, Lee SJ, Kim JH, et al. Effect of the molecular weight of poly(vinyl alcohol) on the water stability of a syndiotactic poly(vinyl alcohol)/iodine complex film. Colloid & Polymer Science 2003;281: 416–22.

[2] Shin EJ, Lee YH, Choi SC. Study on the structure and processability of the iodinated poly(vinyl alcohol). Journal of Applied Polymer Science 2004;91: 2407–15.

[3] Shin EJ, Lyoo WS, Lee YH. Making polyvinyl alcohol films iodinated as solution state before casting and its application. Journal of Applied Polymer Science 2008;109:1143–9.

[4] Song DH, Yoo HY, Lee JJ, Kim JP. Polarizing films based on oriented poly(vinyl alcohol)-dichroic dyes. Molecular Crystals and Liquid Crystals 2006;445: 355–60.

[5] Beekman E, Kocher C, Kokil A, Zimmermann S, Weder C. UV polarizers based on oriented poly(vinyl alcohol)–Chrysophenine–Congo red blend films. Journal of Applied Polymer Science 2002;86:1235–9.

[6] Lyoo WS, Yeum JH, Park JM, Kwak JW, Kim JH, Kim SS, et al. Role of molecular weight of atactic poly(vinyl alcohol) (PVA) in the polarizing efficiency of PVA/ Azo dye complex film with high durability. Journal of Applied Polymer Science 2005;96:967–74.

[7] Song DH, Kim JP. Effect of transition moments and orientational behavior of dichroic dyes on the optical anisotropy of poly(vinyl alcohol) polarizing films. Dyes and Pigments 2009;80:219–25.

[8] Oh SY, Oh JH, Shin DY. Preparation and polarization characteristics of polarizing film using a dichroic azo dye with UV absorbing moiety. Journal of the Korean Institute of Chemical Engineers 2001;39:411–6.

[9] Chang JB, Hwang JH, Park JS, Kim JP. The effect of dye structure on the dyeing and optical properties of dichroic dyes for PVA polarizing film. Dyes and Pigments 2011;88:366–71.

[10] Dirix Y, Tervoort TA, Bastiaansen C. Optical properties of oriented polymer/ dye polarizers. Macromolecules 1995;28:486–91.

[11] CAChe 6.1.8. Beaverton, Oregon: Fujitsu Systems Business of America Inc.

[12] Lye J, Freeman HS, Hinks D. Molecular modeling in dye chemistry: studies involving two disperse dyes. Textile Research Journal 1999;69:583–90.

[13] Goto H, Osawa E. Viewpoint 11 – approaches to the global minimum problem. Journal of Molecular Structure: THEOCHEM 1993;285:157–68.

[14] Ridley JE, Zerner MC. An intermediate neglect of differential overlap technique for spectroscopy: pyrrole and the azines. Theoretica Chimica Acta 1973; 32:111–34.

[15] Kubo Y, Yoshida K, Adachi M, Nakamura S, Maeda S. Experimental and theoretical study of near-infrared absorbing naphthoquinone methide dyes with a nonplanar geometry. Journal of the American Chemical Society 1991; 113:2868–73.

[16] Hanemann T, Böhm MC, Haase W. Calculation of UV/VIS absorption spectra of liquid crystals and dye molecules: an INDO MO approach. Liquid Crystals 1992;11:917–27.

[17] Skrabal P, Zollinger H. Mechanism of azo coupling reactions: part XXXV. pH-dependence and *ortho*/*para* ratio in coupling reactions of amino-hydroxynaphthalenesulfonic acids. Dyes and Pigments 1988;9:201–7.

[18] Gordon PF, Gregory P. Organic chemistry in colour. Springer-Verlag Berlin Heidelberg; 1987. p. 126–95.